

# Lactoferrin improves scopolamine-induced memory impairment in mice

Noa Mizukami<sup>1</sup>, Masayuki Shibuya<sup>1</sup>, Megumi Furukawa<sup>1</sup>, Ryoken Aoki<sup>2</sup>, Kanata Murakami<sup>1</sup>, Masahiro Toho<sup>1</sup>, Daichi Nagashima<sup>3,4</sup>, Nobuo Izumo<sup>1,4,\*</sup>

<sup>1</sup>Laboratory of Pharmacotherapy, Yokohama University of Pharmacy, Yokohama, Kanagawa, Japan;

<sup>2</sup>Center for Pharmaceutical Education, Yokohama University of Pharmacy, Yokohama, Kanagawa, Japan;

<sup>3</sup>Laboratory of Clinical Pharmaceutics, Yokohama University of Pharmacy, Yokohama, Kanagawa, Japan;

<sup>4</sup>General Health Medical Research Center, Yokohama University of Pharmacy, Yokohama, Kanagawa, Japan.

**SUMMARY:** Population aging is increasing worldwide, accompanied by a rising prevalence of cognitive decline and dementia, imposing substantial healthcare and socioeconomic burdens. This study evaluated the effects of lactoferrin on scopolamine-induced memory impairment in 5-week-old ddY mice using the Barnes maze test and the novel object recognition assay to assess cognitive function. Additionally, gene expression levels in the hippocampus were analyzed using reverse transcription-quantitative PCR to explore the underlying mechanisms. Scopolamine impaired spatial and object recognition memory, whereas lactoferrin markedly improved these deficits, with effects comparable to those of donepezil. Scopolamine also increased inflammatory and oxidative stress markers (*Tnf* and *Nos2*) and the apoptosis-related factor (*Casp3*), all of which were attenuated by lactoferrin. These findings indicate that lactoferrin improved scopolamine-induced memory impairment, potentially by suppressing inflammation and oxidative stress, thereby inhibiting neuronal apoptosis. Therefore, lactoferrin may represent a promising functional food component for the prevention of cognitive decline.

**Keywords:** Lactoferrin, scopolamine, memory, *Nos2*, *Casp3*

## 1. Introduction

Population aging is a global issue that not only leads to a decline in the labor force but also increases the risk of various diseases. With advanced age, the likelihood of becoming bedridden increases owing to fractures and muscle weakness. Among central nervous system disorders, dementia is a major concern and is often accompanied by behavioral and psychological symptoms, such as wandering and delusions, which contribute to increasing healthcare costs.

Diseases associated with memory impairment include Alzheimer's disease and Lewy body dementia. Although their etiologies differ, one leading hypothesis is the loss of cholinergic neurons projecting to the limbic system, including the hippocampus. This neuronal loss reduces the amount of acetylcholine released into the synaptic clefts. Consequently, drugs inhibiting cholinesterase, the enzyme responsible for breaking down acetylcholine, are widely used to treat dementia. Nerve cells typically degenerate with age; however, a decrease in acetylcholine has been reported to increase oxidative stress in neurons (1), thereby accelerating neuronal degeneration.

Mouse models are essential for evaluating the efficacy of compounds against memory impairment. While SAMP8 mice exhibit age-related decline, scopolamine-induced models enable rapid and reproducible impairment through cholinergic blockade, making them valuable for pharmacological studies. In addition, numerous studies have used memory impairment models induced by scopolamine, a muscarinic receptor antagonist (2-4). In a previous study, we demonstrated that scopolamine administration caused memory impairment in the Barnes maze test and reported the involvement of oxidative stress associated with increased *Nos2* levels (5). Considering the increasing medical costs associated with the growing number of patients, it is important to focus not only on the pharmacological treatment of dementia but also on its prevention through the daily intake of functional foods and bioactive ingredients.

Lactoferrin (LF) has multiple biological functions, including anti-inflammatory, antibacterial, and antiviral activities, as well as beneficial effects on lipid metabolism (6-8). LF has been widely utilized as a functional food ingredient in Japan (9) and is included

as a functional component under the Food with Function Claims system regulated by the Consumer Affairs Agency. In addition to its role in immune regulation (10), LF has attracted attention owing to its potential effects on the central nervous system. Previous studies have shown that LF enhances analgesic responses and exhibits antidepressant-like effects (11,12). Furthermore, our group has demonstrated that it ameliorates suppression of the serotonergic system in ovariectomized mouse models (13). At the cellular level, LF has been shown to promote neuronal cell growth by activating extracellular signal-regulated kinase signaling in PC12 cells (14). Moreover, accumulating evidence suggests that LF exerts protective effects against tissue damage by suppressing inflammation and oxidative stress, as demonstrated in a model of nonalcoholic steatohepatitis (NASH) (15). Given that oxidative stress is a key contributor to memory impairment, including scopolamine-induced memory impairment, these findings suggest that LF may exert protective effects against cognitive dysfunction.

Therefore, we hypothesized that LF would attenuate scopolamine-induced cognitive impairment through neuroprotective mechanisms that suppress oxidative stress, neuroinflammation, and neuronal cell death-related signaling pathways. To test this hypothesis, we investigated the effects of LF on cognitive function and markers associated with neuroprotective pathways in a scopolamine-induced mouse model.

## 2. Materials and Methods

### 2.1. Animals

We employed 5-week-old ddY male mice purchased from SLC Inc. (Shizuoka, Japan). The animals were housed under controlled conditions ( $24 \pm 1^\circ\text{C}$  and 55% humidity) and maintained on a 12-h light/12-h dark cycle (light period, 07:00-19:00, dark period, 19:00-07:00). The animals were fed a standard rodent diet (Labo MR Stock; Nosan, Kanagawa, Japan) and provided tap water *ad libitum*. All experiments were conducted in accordance with the Guidelines for the Proper Conduct of Animal Experiments (Science Council of Japan) and were approved by the Yokohama University of Pharmacy (2023-014).

The mice were allocated to four experimental groups: control ( $n = 24$ ), scopolamine hydrobromide trihydrate (SCOP;  $n = 24$ ), SCOP + LF ( $n = 24$ ), and SCOP + donepezil hydrochloride (DNP;  $n = 14$ ). Behavioral experiments were conducted in three independent experimental batches owing to limitations in the number of animals that could be assessed simultaneously. The control, SCOP, and SCOP + LF groups were included in all three batches, whereas the SCOP + DNP group was included only in the second and third batches. As a result, the number of animals in the SCOP + DNP group was lower than that in the other groups. RT-qPCR analysis

was performed using hippocampal tissues obtained from animals in the second and third experimental batches. This strategy enabled all samples to be analyzed under identical experimental conditions and minimized inter-assay variability.

After a 7-day acclimation period, behavioral training was initiated when the mice were approximately 6 weeks old. Following the 3-day training period, mice received the assigned treatments for 21 days. Behavioral testing and tissue collection were subsequently performed at 9–10 weeks of age (Figure 1).

### 2.2. Administration of experimental compounds

SCOP and DNP were purchased from Tokyo Chemical Industry Co., Ltd. (Tokyo, Japan). Bovine LF was obtained from NRL Pharma, Inc. (Tokyo, Japan). SCOP was diluted in physiological saline (0.9% w/v NaCl), and LF and DNP were diluted in tap water. Animals were administered SCOP (5 mg/kg) *via* intraperitoneal injection, and LF (300 mg/kg) and DNP (3 mg/kg) were administered orally. Administration was performed for 21 consecutive days, beginning the day after completion of the Barnes maze training period. On the day of behavioral testing or necropsy, experimental compounds were administered 1 h before the respective procedure. The doses were selected based on our previous experimental findings and published evidence (5).

### 2.3. Barnes maze test

The Barnes maze test was performed as described in our previous study (5). The Barnes maze test was conducted using an MB-10 apparatus (SHINFACTORY, Fukuoka, Japan). The apparatus consisted of a circular platform measuring 455 mm in diameter and 920 mm in height, with 20 holes (25 mm diameter) located 30 mm from the edge. The escape box measured 130 mm  $\times$  95 mm  $\times$  50 mm (width  $\times$  depth  $\times$  height). The light intensity was maintained at 600–700 Lx as a weakly aversive stimulus. To prevent interference with learning, the maze was enclosed by partitions, and three visual cues (stars, triangles, and double-circle shapes) were attached to the partitions. To prevent the use of olfactory cues and maze orientation for task performance, the platform was rotated  $90^\circ$  after each trial. The maze and associated apparatus were cleaned with 70% ethanol after each trial. All procedures were recorded using a high-definition digital camera (HC-W580M; Panasonic, Tokyo, Japan). The Barnes maze test consisted of three phases: habituation, repeated learning training, and probe testing.

#### 2.3.1. Habituation

The habituation phase was conducted one day prior to the repeated learning test. During habituation, the

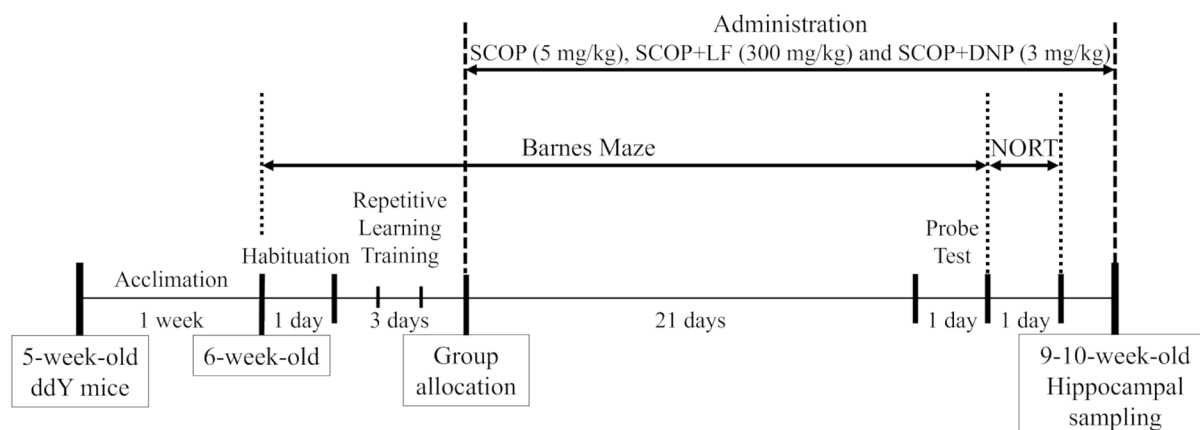


**Figure 1. Experimental timeline of the study.** Timeline of the experimental procedures, including behavioral assessments, experimental compound administration, and tissue collection. Following a 1-week acclimation period, 6-week-old male ddY mice were evaluated using the Barnes Maze test. The Barnes maze protocol consisted of a 1-day habituation phase followed by 3 days of repeated learning training. Mice were assigned to experimental groups based on their performance during the training period. Experimental compound administration began the day after completion of the Barnes maze training period and continued for 21 days. A probe test was conducted after the treatment period to assess spatial memory retention, followed by the NORT the following day. Hippocampal tissues were subsequently collected for molecular analyses. NORT, novel object recognition test; SCOP, scopolamine hydrobromide trihydrate (5 mg/kg); SCOP + LF, SCOP plus lactoferrin (300 mg/kg); SCOP + DNP, SCOP plus donepezil hydrochloride (3 mg/kg).

maze board was used without visual cues or an escape box, allowing the mice to explore freely for 120 s. Subsequently, each mouse was placed in the center of the maze and confined within a transparent beaker for 20 s, after which the escape box was introduced. The mouse was then guided into the escape box, with the hole blocked with an opaque weight, and remained there for 60 s. This procedure was performed once for each mouse.

### 2.3.2. Repetitive learning training

Repeated learning training was conducted for three consecutive days beginning the day after the habituation phase. During repeated learning training, the visual cues were displayed, and the escape box was positioned beneath the target hole. Mice were confined for 20 s in a start box (a light-proof white cylinder; 9.7 cm in diameter and 13.2 cm in height) positioned at the center of the maze. The start box was then removed, and each mouse was allowed to freely explore the maze for up to 120 s. During this time, the latencies to locate and enter the escape box were recorded independently. If a mouse did not enter the escape box within the allotted time, it was guided to the escape box. Upon entering the escape box, the mouse was confined for 60 s. After completion of the training period, the learning rate was calculated by dividing the mean escape box arrival latency on day 3 by that on day 1. Prior to treatment allocation, animals were assigned to four groups (control, SCOP, SCOP + LF, and SCOP + DNP), and no significant differences in learning rate were observed among the groups.

### 2.3.3. Probe test

The probe test was conducted 21 days after completion of repeated learning training. During the probe test, visual cues were present, whereas the escape box was removed. The mice were confined in the start box at the center of the maze for 20 s, after which they were allowed to explore the maze freely for 120 s. Behavior was recorded using a camera positioned directly above the maze. This procedure was performed once for each mouse. Only the first 60 s of the recorded behavior were included in the analysis. The maze board was divided into four zones: the area around the escape box and associated star-shaped visual cue was designated ZONE1; the area surrounding the triangle-shaped visual cue was designated ZONE2; the area surrounding the double-circle visual cue was designated ZONE3; and the area without visual cues was designated ZONE4. The time spent in each zone and the proportion of total distance traveled within each zone were measured to evaluate spatial memory.

### 2.4. Novel object recognition test (NORT)

The NORT was performed as previously described (16,17). This experiment was conducted in an open-field apparatus (50 × 50 × 30 cm high) under a light intensity of 25–50 lx. Two objects of similar height were selected: object A (8.2 cm in diameter, 9.7 cm in height; white cylinder) and object B (6.5 cm in diameter, 8.9 cm in height; gray cylinder), which differed in color and shape. The object was placed along the diagonal axis within the central 25 × 25 cm area of the open field. To minimize the influence of olfactory or positional cues, object positions were swapped for each mouse. The maze and objects were cleaned with 70% ethanol between trials. All procedures were recorded using a high-definition

digital camera. The NORT consisted of three phases: habituation, familiarization (T1), and testing (T2), with experimental compounds administered 1 h before each phase.

During habituation, mice were allowed to freely explore the open field for 10 min in the absence of objects. Familiarization (T1) was conducted the day after habituation. During T1, two identical objects were placed, and each mouse was released into the center of the arena and allowed to explore freely for 10 min. T2 was conducted 1 h after T1. During T2, one of the identical objects used in T1 was placed at the same location as during T1, whereas the other object was replaced with a novel object and positioned at the corresponding location. Mice were released into the center of the open field and allowed to explore freely for 10 min. Only the first 5 min of the exploration period were included in the analysis. The duration and frequency of object exploration were recorded for each object. For the novel object, the exploration duration and exploration frequency were each divided by the corresponding total value for the familiar and novel objects combined, and the resulting values were expressed as percentages. Two animals in the SCOP + DNP group died during the oral administration period owing to an inadvertent gavage-related technical error and were excluded from the NORT analysis.

### 2.5. Reverse transcription-quantitative PCR (RT-qPCR)

The hippocampus was dissected from mouse brains, and total RNA was extracted using ISOGEN (Nippon Gene, Tokyo, Japan). Tissue homogenization was performed using a Polytron PT 1300 D homogenizer (Kinematica AG, Lucerne, Switzerland). Complementary DNA (cDNA) was synthesized using PrimeScript™ RT Master Mix (Takara Bio Inc., Shiga, Japan) with the extracted RNA as a template. The reaction mixture was incubated at 37°C for 15 min, followed by incubation at 85°C for 5 s.

**Table 1. Primer sequences**

Gene	Sequences (5'→3')
<i>Gapdh</i>	Forward: AGCTTGTTCATCAACGGGAAG Reverse: TTTGATGTTAGTGGGGTCTCG
<i>Tnf</i>	Forward: CCTCTTCTCATTCTGCTTG Reverse: GCCATTTGGGAAGTCTCATCC
<i>Il1b</i>	Forward: AGTTGACGGACCCAAAAG Reverse: AGCTGGATGCTCTCATCAGG
<i>Ccl2</i>	Forward: GGGACACTGGCTGCTTGT Reverse: GTTGTTAAGCAGAAGATTCACGTC
<i>Nos2</i>	Forward: CTTTGCCACGGACGAGAC Reverse: TCATTGTAAGTCTGAGGGCTGAC
<i>Trp53</i>	Forward: CCAGGATGTTGCAGAGTTGTT Reverse: GCAGGAGCTGACACTTGA
<i>Casp3</i>	Forward: GAGGCTGACTTCTGTATGCTT Reverse: AACCCAGCCCGTCTTT
<i>Bdnf</i>	Forward: AGTCTCCAGGACAGCAAAGC Reverse: TGCAACCGAAGTATGAAATAACC

RT-qPCR was performed using the LightCycler® 96 System (Hoffmann-La Roche, Basel, Switzerland) with SYBR GREEN I MASTER Mix (Hoffmann-La Roche, Basel, Switzerland), and amplification was monitored using the intercalation method. The qPCR cycling conditions consisted of an initial denaturation step at 95°C for 10 min, followed by 40–50 amplification cycles of 95°C for 10 s (denaturation) and 60°C for 20–30 s (annealing/extension).

Gene expression levels were calculated relative to those of *Gapdh*. The PCR primer sequences are listed in Table 1.

### 2.6. Statistical analysis

For group comparisons, data from repeated learning training were analyzed using a linear mixed-effects model (LMM), whereas other data were analyzed using Dunnett's test. Statistical analysis was performed using the free statistical software EZR (v.1.68; Jichi Medical University, Tochigi, Japan) (18). Significance levels were set at  $p < 0.001$ ,  $p < 0.05$ , and  $p < 0.01$ .

## 3. Results

### 3.1. Barnes maze test

The Barnes maze test was used to evaluate hippocampus-dependent spatial learning and long-term memory. Figure 2 shows the latency to enter the target hole during repetitive learning training (Figure 2). LMM analysis revealed no significant differences among the experimental groups, indicating comparable baseline performance prior to treatment allocation.

Three weeks after the initiation of experimental compound administration, a probe test was conducted.

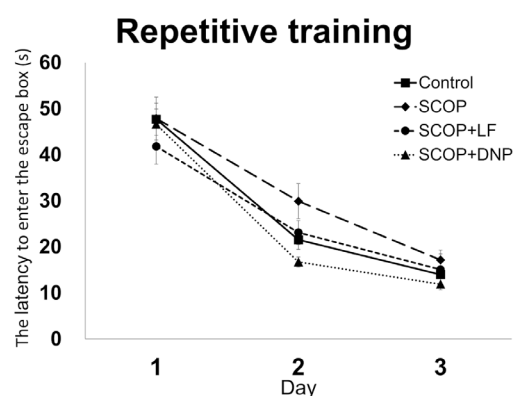


**Figure 2. Baseline learning performance during the 3-day repeated learning training period used for group allocation.** Linear mixed-effects model (LMM) analysis shows no significant between-group differences in learning rates during the repeated learning test. Data are presented as mean ± SEM (control, SCOP, and SCOP + LF:  $n = 24$ , SCOP + DNP:  $n = 14$ ). SCOP, scopolamine hydrobromide trihydrate (5 mg/kg); SCOP + LF, SCOP plus lactoferrin (300 mg/kg); SCOP + DNP, SCOP plus donepezil hydrochloride (3 mg/kg).

The time spent in each zone and the percentage of distance traveled are presented in Figures 3A–3C. In ZONE1, where the target hole was located, the time spent was significantly decreased in the SCOP group ( $13.4 \pm 1.3\%$ ) compared with the control group ( $23.9 \pm 1.5\%$ ), whereas it was significantly increased in the SCOP + DNP group ( $22.0 \pm 2.9\%$ ) compared with the SCOP group (Figure 3B). These findings support the successful establishment of the scopolamine-induced memory impairment model. The SCOP + LF group ( $22.5 \pm 2.1\%$ ) also exhibited a significant increase compared with the SCOP group. In ZONE3, which is located diagonally opposite ZONE1, the control and SCOP + LF groups spent significantly less time than the SCOP group.

In ZONE1, the percentage of distance traveled was significantly reduced in the SCOP group ( $25.0 \pm 2.3\%$ ) compared with the control group ( $36.7 \pm 2.1\%$ ), whereas it was significantly increased in the SCOP + LF group ( $35.6 \pm 3.0\%$ ) compared with the SCOP group (Figure 3C). Furthermore, consistent with the findings for time spent in each zone (Figure 3B), both the control and SCOP + LF groups showed a significantly lower

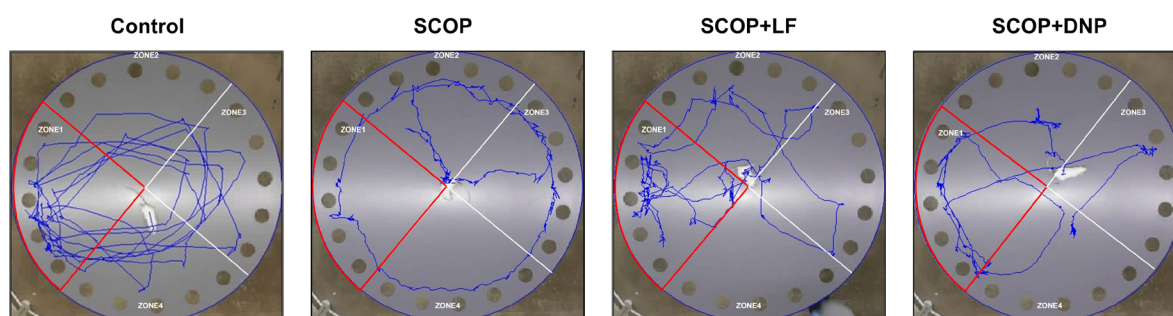
percentage of distance traveled in ZONE3 than the SCOP group.

### 3.2. NORT

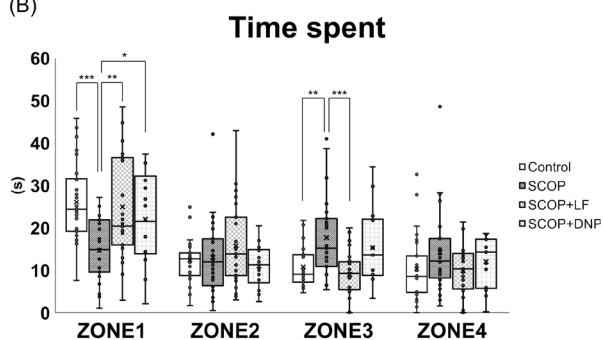
The NORT was conducted to evaluate short-term object recognition memory (Figure 4A). During the familiarization phase (T1), in which two identical objects were presented, both the object exploration duration (%) (Figure 4B) and object exploration frequency (%) (Figure 4C) were approximately 50% across all groups, indicating no object preference (Figure 4B and 4C). These results confirmed that the experimental conditions for NORT were appropriately established.

During the test phase (T2), conducted 1 h after T1, one of the familiar objects was replaced with a novel object. The novel object exploration duration (%) was significantly lower in the SCOP group than in the control group and significantly higher in the SCOP + DNP group than in the SCOP group (Figure 4B). In addition, the SCOP + LF group exhibited a significant increase in the novel object exploration duration (%) compared with the SCOP group (Figure 4B). In contrast, novel object

(A)



(B)



(C)

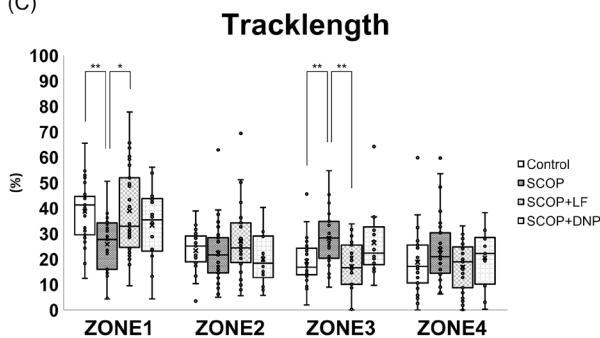


**Figure 3. Effect of 3-week experimental compound administration on Barnes maze performance.** (A) Representative movement trajectories during the probe test for each group (control, SCOP, SCOP + LF, and SCOP + DNP), illustrating differences in spatial exploration patterns. ZONE1 (red frame) corresponds to the area surrounding the former location of the escape box. (B) Time spent and (C) percentage of distance traveled in each zone during the Barnes maze probe test across experimental groups. Data are presented as box-and-whisker plots. The center line indicates the median, the box represents the interquartile range (25th–75th percentiles), and the whiskers indicate the minimum and maximum values (control, SCOP, and SCOP + LF:  $n = 24$ , SCOP + DNP:  $n = 14$ ). Statistical analysis was performed using Dunnett's test. \* $p < 0.05$ , \*\* $p < 0.01$ , and \*\*\* $p < 0.001$  versus SCOP. SCOP, scopolamine hydrobromide trihydrate (5 mg/kg); SCOP + LF: SCOP plus lactoferrin (300 mg/kg); SCOP + DNP, SCOP plus donepezil hydrochloride (3 mg/kg).

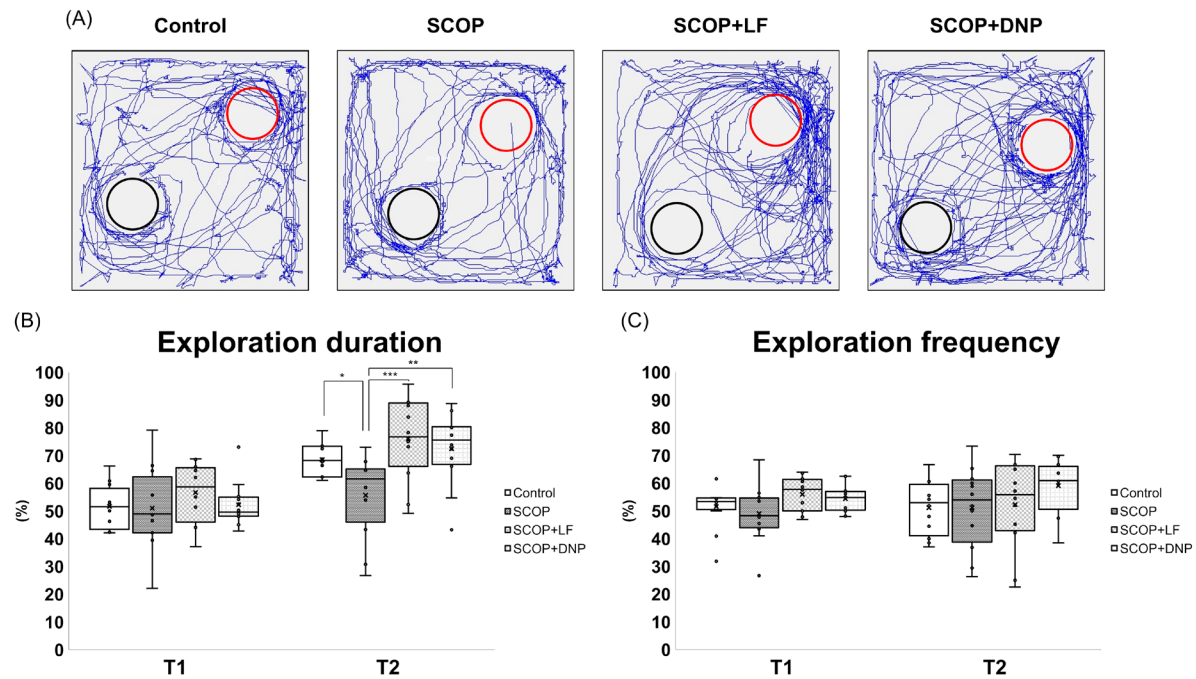


**Figure 4. Effects of experimental compound administration on short-term object recognition memory assessed 1 h after administration.** (A) Representative movement trajectories during the T2 in each group (control, SCOP, SCOP + LF, and SCOP + DNP), illustrating differences in spatial exploration behavior. Red circles indicate the novel object, while black circles indicate the familiar object used in T1. (B) Novel object exploration (%) and (C) novel object exploration frequency (%) in T1 and T2 of the novel object recognition test. Data are presented as box-and-whisker plots. The center line indicates the median, the box represents the interquartile range (25th–75th percentiles), and the whiskers indicate the minimum and maximum values (control, SCOP, and SCOP + LF:  $n = 24$ , SCOP + DNP:  $n = 14$ ). Statistical analysis was performed using Dunnett's test. \* $p < 0.05$ , \*\* $p < 0.01$ , and \*\*\* $p < 0.001$  versus SCOP. SCOP, scopolamine hydrobromide trihydrate (5 mg/kg); SCOP + LF: SCOP plus lactoferrin (300 mg/kg); SCOP + DNP, SCOP plus donepezil hydrochloride (3 mg/kg).

exploration frequency (%) did not differ significantly among the groups (Figure 4C).

### 3.3. Effects of experimental compound administration on hippocampal gene expression

To evaluate the effects of the experimental compounds on hippocampal gene expression, mRNA expression levels of inflammatory mediators *Tnf*, *Il1b*, and *Ccl2*, as well as *Nos2*, a key enzyme involved in inflammation-associated nitric oxide production, were analyzed. Furthermore, *Bdnf*, a key regulator of neuronal survival and synaptic plasticity, and the apoptosis-related factors *Trp53* and *Casp3* were examined.

*Tnf* expression was significantly elevated in the SCOP group compared with the control group, and this increase was significantly attenuated in the SCOP + LF and SCOP + DNP groups (Figure 5A). In contrast, *Il1b* and *Ccl2* expression levels did not differ significantly among the groups (Figures 5B and 5C). Similarly, *Nos2* expression was significantly elevated in the SCOP group, and this increase was significantly attenuated in the SCOP + LF and SCOP + DNP groups (Figure 5D). No significant differences were observed in *Bdnf* expression levels among the groups (Figure 6A). In addition, no significant differences in *Trp53* expression levels were observed between the SCOP, control, and SCOP + DNP

groups. However, *Trp53* expression was significantly reduced in the SCOP + LF group (Figure 6B). Conversely, *Casp3* expression was significantly elevated in the SCOP group, and this increase was significantly attenuated in the SCOP + LF and SCOP + DNP groups (Figure 6C).

## 4. Discussion

Our findings demonstrate that oral LF administration ameliorated scopolamine-induced memory impairment. This study was performed using a murine model of memory impairment induced by scopolamine, a muscarinic receptor antagonist. Our previous study demonstrated that scopolamine administration after repeated training induced memory impairment in the Barnes maze test (5). Moreover, we previously reported that SAMP8 mice, a model of accelerated aging, exhibit impaired performance during repeated learning in the Barnes maze test (19). Therefore, in the present study, mice were assigned to experimental groups based on their performance during the 3-day training period to ensure comparable baseline learning ability and minimize differences in memory consolidation among the groups. Following the 3-day training period, mice received scopolamine alone, scopolamine plus donepezil, or scopolamine plus LF for three weeks. In the probe test

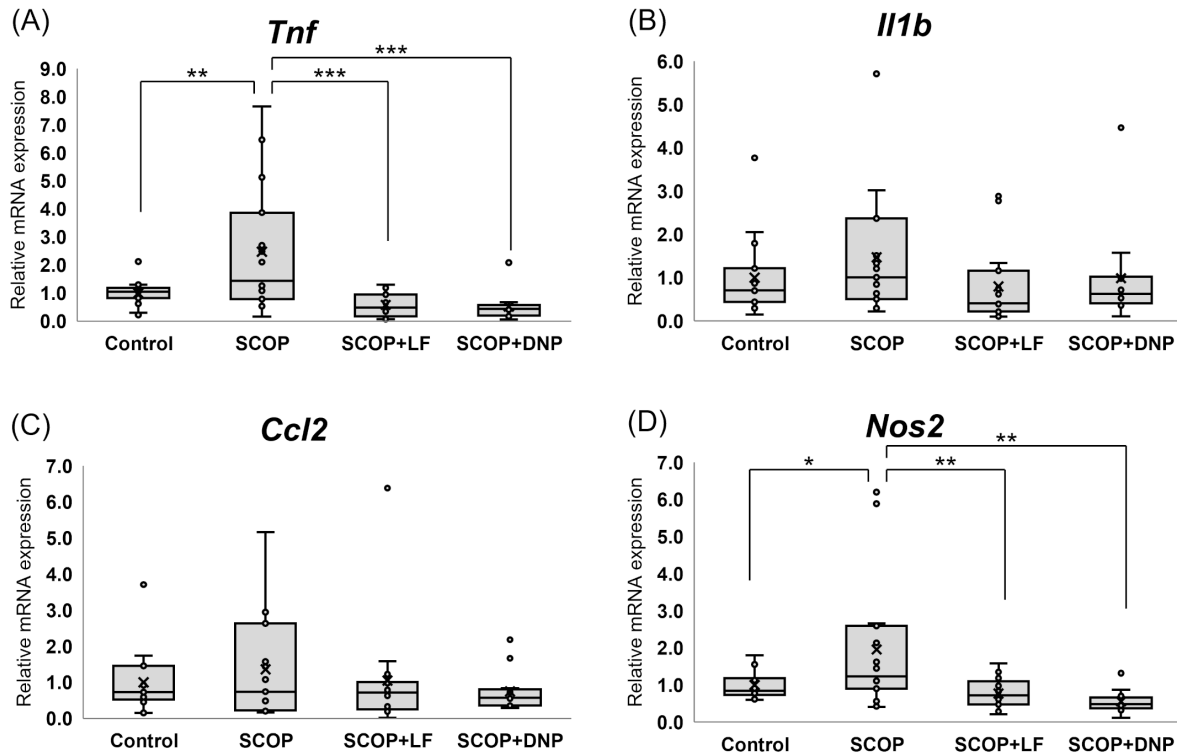


**Figure 5. Effects of experimental compound administration on hippocampal mRNA expression of *Tnf*, *Il1b*, *Ccl2*, and *Nos2*.** Hippocampal mRNA expression of inflammation- and oxidative stress-related genes. (A) *Tnf*, (B) *Il1b*, (C) *Ccl2*, and (D) *Nos2*, as quantified by RT-qPCR. Data are presented as box-and-whisker plots. The center line indicates the median, the box represents the interquartile range (25th–75th percentiles), and the whiskers indicate the minimum and maximum values (control, SCOP, and SCOP + LF:  $n = 24$ , SCOP + DNP:  $n = 14$ ). Statistical analysis was performed using Dunnett's test. \* $p < 0.05$ , \*\* $p < 0.01$ , and \*\*\* $p < 0.001$  versus SCOP. SCOP, scopolamine hydrobromide trihydrate (5 mg/kg); SCOP + LF: SCOP plus lactoferrin (300 mg/kg); SCOP + DNP, SCOP plus donepezil hydrochloride (3 mg/kg).

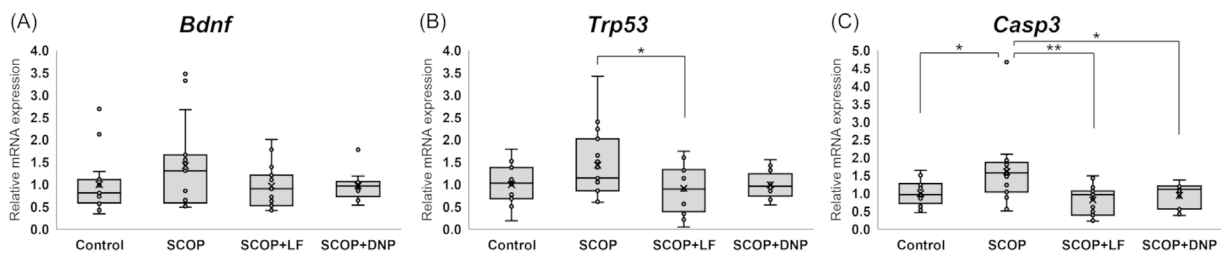


**Figure 6. Effects of experimental compound administration on hippocampal mRNA expression of *Bdnf*, *Trp53*, and *Casp3*.** Hippocampal mRNA expression levels of (A) *Bdnf*, a gene associated with neuronal survival and synaptic plasticity, and the apoptosis-related genes (B) *Trp53* and (C) *Casp3*, as quantified by RT-qPCR. Data are presented as box-and-whisker plots. The center line indicates the median, the box represents the interquartile range (25th–75th percentiles), and the whiskers indicate the minimum and maximum values (control, SCOP, and SCOP + LF:  $n = 24$ , SCOP + DNP:  $n = 14$ ). Statistical analysis was performed using Dunnett's test. \* $p < 0.05$ , \*\* $p < 0.01$ , and \*\*\* $p < 0.001$  versus SCOP. SCOP, scopolamine hydrobromide trihydrate (5 mg/kg); SCOP + LF: SCOP plus lactoferrin (300 mg/kg); SCOP + DNP, SCOP plus donepezil hydrochloride (3 mg/kg).

conducted after the treatment period, the control group demonstrated sustained memory retention, spending approximately 24% of the test time in ZONE1 even two weeks after training. In contrast, the scopolamine-only group spent only 13% of the test time in ZONE1, indicating impaired memory retention.

Cholinergic neurons projecting from the Meynert basal nucleus to the hippocampus and other brain regions are involved in memory processes, and scopolamine

induces memory impairment by blocking muscarinic receptors (20). Accordingly, we postulated that the scopolamine-induced memory impairment was mediated, at least in part, through this pathway. In this study, donepezil, a cholinesterase inhibitor widely used for the treatment of Alzheimer's disease, markedly improved memory impairment, suggesting that restoration of cholinergic neurotransmission can counteract the effects of scopolamine-induced muscarinic receptor blockade.

Although LF does not possess cholinesterase-inhibitory activity, it produced a comparable improvement in memory impairment. Analysis of trajectories in each region during the probe test revealed that activity in the region opposite to the target region was significantly reduced in the LF group. In contrast, the donepezil group exhibited a more uniform distribution of activity across the three non-target regions, suggesting that donepezil may improve memory performance through distinct underlying mechanisms.

In the NORT (T2), the scopolamine-only group demonstrated a novel object exploration duration (%) of approximately 50%, suggesting impaired short-term recognition memory. In contrast, the LF and donepezil groups exhibited novel object exploration durations of  $\geq 70\%$ , suggesting that these treatments improved short-term memory impairment. Notably, no significant differences were observed in novel object exploration frequency (%) among the groups, supporting the validity of the object recognition memory test. To investigate the mechanisms underlying the LF-mediated effects on memory, hippocampal gene expression levels were analyzed by RT-qPCR. Scopolamine administration has been shown to induce inflammation *via* muscarinic receptor blockade (21,22). In addition, scopolamine administration has been reported to markedly increase *Nos2* levels, which are associated with oxidative stress (5). LF has been reported to exert anti-inflammatory effects in immune cells (23), and our previous study using a NASH mouse model demonstrated its ability to suppress hepatic inflammation (15). In addition, LF has been reported to possess antioxidant properties (24). To investigate the effects of scopolamine-induced inflammation in the hippocampus, we examined the expression of *Tnf*, *Il1b*, and *Ccl2*. Scopolamine administration markedly increased *Tnf* expression, whereas LF and donepezil significantly suppressed this increase, suggesting anti-inflammatory effects. TNF- $\alpha$  is a proinflammatory cytokine produced primarily by macrophages. Liu *et al.* (2022) reported that LF exerts anti-inflammatory effects by modulating macrophage function (25), raising the possibility that a similar mechanism may also operate in the hippocampus. In the central nervous system, microglia perform functions analogous to those of macrophages; therefore, LF may exert anti-inflammatory effects through the modulation of microglial activity. Our previous study using a NASH mouse model demonstrated that LF suppresses inflammation through effects on hepatic macrophages, and the findings of the present study further support the anti-inflammatory properties of LF. In contrast, although *Il1b* demonstrated a trend similar to that of *Tnf*, no statistically significant difference was observed. Likewise, no significant differences were observed in the expression of *Ccl2*, a chemokine involved in macrophage migration. One possible explanation for this finding is that hippocampal tissue was collected 24

h after the final dose. Next, we examined the expression of *Nos2*, which encodes inducible nitric oxide synthase (iNOS), a key enzyme involved in inflammation-associated oxidative stress. iNOS catalyzes the production of nitric oxide, which activates soluble guanylate cyclases. In turn, reactive oxygen and nitrogen species induce *Nos2* expression, establishing a positive feedback loop. Thus, *Nos2* upregulation may contribute to the exacerbation of oxidative stress. Scopolamine markedly increased the expression of *Nos2*, whereas LF or donepezil substantially inhibited this increase. Likewise, our previous study demonstrated that scopolamine increases oxidative stress (5). Furthermore, scopolamine has been reported to enhance oxidative stress by inhibiting superoxide dismutase activity (26); however, the mechanisms underlying scopolamine-induced oxidative stress remain to be fully elucidated. Because LF suppressed the scopolamine-induced increase in oxidative stress, we next examined the expression of *Bdnf*, a key regulator of neuronal survival and synaptic plasticity, as well as the apoptosis-related genes *Trp53* and *Nos2*. Although *Bdnf* expression did not differ significantly among the groups, it tended to increase in the scopolamine group and decrease following LF treatment. Elevated BDNF levels promote nerve growth, whereas oxidative stress is generally thought to inhibit this process. However, despite the increase in oxidative stress induced by scopolamine, *Bdnf* expression tended to increase in the present study. One possible explanation is that the relatively young age of the mice (approximately 10 weeks old) elicited a feedback mechanism. Wu *et al.* (2020) reported that BDNF suppression contributed to neuronal loss in 24-week-old mice (27), suggesting that age may influence the relationship between oxidative stress and *Bdnf* expression. The scopolamine-treated group exhibited a trend toward increased *Trp53* expression and a significant increase in *Casp3* expression. This suggests that scopolamine induces inflammation by activating macrophages and promotes neuronal cell death by increasing oxidative stress. Because LF markedly suppressed these changes, it may reduce oxidative stress in neurons and exert anti-inflammatory effects by modulating microglial activity.

The beneficial effects of LF on cognitive function have previously been reported in aged mice and *APP/PS1* transgenic mouse models (28,29). Consistent with these findings, the present study demonstrated that LF improves memory performance. However, unlike previous studies, we employed a scopolamine-induced cognitive impairment model, which is widely used to mimic cholinergic dysfunction-associated memory deficits. Furthermore, the beneficial effects of orally administered LF were associated with the reduced expression of *Tnf*, *Nos2*, *Trp3*, and *Casp3*. Accordingly, LF may ameliorate cognitive impairment by modulating neuroinflammatory, oxidative stress-related, and

apoptosis-related pathways during cholinergic dysfunction.

These results indicate that LF improves scopolamine-induced memory impairment by inhibiting neuronal loss *via* its anti-inflammatory and antioxidant effects.

### Acknowledgements

We thank NRL Pharma for providing the lactoferrin. The authors would like to thank Editage for English language editing.

*Funding:* None.

*Conflict of Interest:* The authors have no conflicts of interest to disclose.

### References

- Wal P, Dutta A, Jawaid T, *et al.* Synaptic aging and neurodegeneration: the role of synaptic vesicle dynamics and neurotransmitter imbalance. *Biogerontology*. 2026; 27:55.
- Zavala-Ocampo LM, López-Camacho PY, Aguirre-Hernández E, Cárdenas-Vázquez R, Bonilla-Jaime H, Basurto-Islas G. Neuroprotective effects of *Petiveria alliacea* on scopolamine-induced learning and memory impairment mouse model. *J Ethnopharmacol*. 2024; 318:116881.
- Kim SS, Kim WS, Moon H, Oh SJ, Hong GS, Lee B, Choi CW, Lee B, Choi JS, Kim MS. 3',4',7-trihydroxyflavone activates the CREB-BDNF axis and restores scopolamine-induced memory deficit in mice. *Eur J Pharmacol*. 2025; 999:177645.
- Jee SC, Lee KM, Kim M, Lee YJ, Kim S, Park JO, Sung JS. Neuroprotective effect of *Cudrania tricuspidata* fruit extracts on scopolamine-induced learning and memory impairment. *Int J Mol Sci*. 2020; 21:9202.
- Ishiyama Y, Furukawa M, Toho M, Aoki R, Fujimura R, Shibuya M, Sato K, Nagashima D, Izumo N. The Barnes maze test is useful for evaluating scopolamine-induced memory impairment model mice. *Pharmacometrics*. 2025; 108:169-176.
- Rosa L, Ianiro G, Conte AL, Conte MP, Ottolenghi L, Valenti P, Cutone A. Antibacterial, anti-invasive, and anti-inflammatory activity of bovine lactoferrin extracted from milk or colostrum versus whole colostrum. *Biochem Cell Biol*. 2024; 102:331-341.
- Ding L, Chen JS, Xing YF, Li DM, Fu AQ, Tong X, Chen GC, Xu JY, Qin LQ. Effects of lactoferrin on high-fat and high-cholesterol diet-induced non-alcoholic fatty liver disease in mice. *J Nutr Biochem*. 2025; 143:109938.
- Rizzi M, Manzoni P, Germano C, Quevedo MF, Sainaghi PP. Lactoferrin, a natural protein with multiple functions in health and disease. *Nutrients*. 2025; 17:3403.
- Ueno H. Applications of lactoferrin as a functional food ingredient. *Jpn J Dairy Sci*. 2012; 61:105-110.
- Berlutti F, Pantanella F, Natalizi T, Frioni A, Paesano R, Polimeni A, Valenti P. Antiviral properties of lactoferrin -- a natural immunity molecule. *Molecules*. 2011; 16:6992-7018.
- Fujimura T, Iguchi A, Sato A, Kagaya S, Hoshino T, Takeuchi T. The pain-relieving effects of lactoferrin on oxaliplatin-induced neuropathic pain. *J Vet Med Sci*. 2020; 82:1648-1654.
- Ahmed HH, Essam RM, El-Yamany MF, Ahmed KA, El-Sahar AE. Unleashing lactoferrin's antidepressant potential through the PI3K/Akt/mTOR pathway in chronic restraint stress rats. *Food Funct*. 2023; 14:9265-9278.
- Izumo N, Yukiko I, Kagaya N, Furukawa M, Iwasaki R, Sumino A, Hayamizu K, Nakano M, Hoshino T, Kurono H, Watanabe Y, Manabe T. Lactoferrin suppresses decreased locomotor activities by improving dopamine and serotonin release in the amygdala of ovariectomized rats. *Curr Mol Pharmacol*. 2021; 14:245-252.
- Nagashima D, Mizukami N, Ogawa N, Suzuki S, Ohno M, Aoki R, Furukawa M, Izumo N. Bovine lactoferrin promotes neurite outgrowth in PC12 cells *via* the TrkA receptor. *Int J Mol*. 2024; 25:11249.
- Aoki R, Ishido K, Furukawa M, Ishibashi Y, Nozaki S, Ito N, Toho M, Nagashima D, Izumo N. Bovine lactoferrin intake prevents hepatic injury in a mouse model of non-alcoholic steatohepatitis induced by choline and methionine deficiency. *Drug Discov Ther*. 2025; 19:230-236.
- Ennaceur A. One-trial object recognition in rats and mice: methodological and theoretical issues. *Behav Brain Res*. 2010; 215:244-254.
- Lueptow LM. Novel object recognition test for the investigation of learning and memory in mice. *J Vis Exp*. 2017; 30:55718.
- Kanda Y. Investigation of the freely available easy-to-use software 'EZ' for medical statistics. *Bone Marrow Transplant*. 2013; 48:452-458.
- Mima Y, Izumo N, Chen JR, Yang SC, Furukawa M, Watanabe Y. Effects of *Coriandrum sativum* seed extract on aging-induced memory impairment in Samp8 mice. *Nutrients*. 2020; 12:455.
- Bartus RT, Dean RT 3rd, Beer B, Lippa AS. The cholinergic hypothesis of geriatric memory dysfunction. *Science*. 1982; 217:408-414.
- Falsafi SK, Deli A, Höger H, Pollak A, Lubec G. Scopolamine administration modulates muscarinic, nicotinic and NMDA receptor systems. *PLoS One*. 2012; 7:e32082.
- Cheon SY, Koo BN, Kim SY, Kam EH, Nam J, Kim EJ. Scopolamine promotes neuroinflammation and delirium-like neuropsychiatric disorder in mice. *Sci Rep*. 2021; 11:8376.
- Cutone A, Rosa L, Lepanto MS, Scotti MJ, Berlutti F, Bonaccorsi di Patti MC, Musci G, Valenti P. Lactoferrin efficiently counteracts the inflammation-induced changes of the iron homeostasis system in macrophages. *Front Immunol*. 2017; 8:705.
- Guan S, Lu S, Zhang R, Wang Y, Yao X, Deng X, Lu J. Lactoferrin alleviates LPS-induced oxidative stress and necroptosis in liver by promoting mitophagy. *J Agric Food Chem*. 2025; 73:11948-11959.
- Liu C, Peng Q, Wei L, Li Z, Zhang X, Wu Y, Wang J, Zheng X, Wen Y, Zheng R, Yan Q, Ye Q, Ma J. Deficiency of Lactoferrin aggravates lipopolysaccharide-induced acute inflammation *via* recruitment macrophage in mice. *Biometals*. 2023; 36:549-562.
- Zhang Q, Li Y, Fan B, Wang F, Li Z, Pires Dias AC, Liu X, Wang Q. *Dendrobium nobile* Lindl ameliorates learning and memory deficits in scopolamine-treated mice. *J Ethnopharmacol*. 2024; 324:117416.
- Wu SY, Pan BS, Tsai SF, Chiang YT, Huang BM, Mo

- FE, Kuo YM. BDNF reverses aging-related microglial activation. *J Neuroinflammation*. 2020; 17:210.
28. Abdelhamid M, Jung CG, Zhou C, Abdullah M, Nakano M, Wakabayashi H, Abe F, Michikawa M. Dietary lactoferrin supplementation prevents memory impairment and reduces amyloid- $\beta$  generation in J20 mice. *J Alzheimers Dis*. 2020; 74:245-259.
29. Zheng J, Xie Y, Li F, Zhou Y, Qi L, Liu L, Chen Z. Lactoferrin improves cognitive function and attenuates brain senescence in aged mice. *J Funct Foods*. 2020; 65:103736.

Received May 6, 2026; Revised June 19, 2026; Accepted June 20, 2026.

*\*Address correspondence to:*

Nobuo Izumo, Laboratory of Pharmacotherapy, Yokohama University of Pharmacy, 601 Matano-cho, Totsuka-ku, Yokohama, Kanagawa 245-0066, Japan.

E-mail: n.izumo@hamayaku.ac.jp

Released online in J-STAGE as advance publication June 25, 2026.